Full Flight Envelope Inner-Loop Control Law Development for the Unmanned K-MAX®

Mohammadreza H. Mansur
Mark B. Tischler
Aeroflightdynamics Directorate (AMRDEC)
US Army RDEC
Ames Research Center
Moffett Field, CA, USA

Michael D. Bielefield
James W. Bacon
Kaman Aerospace Corporation
Bloomfield, CT, USA

Kenny K. Cheung
Marcos G. Berrios
Keith E. Rothman
University Affiliated Research Center (UARC)
University of California, Santa Cruz
Moffett Field, CA, USA

ABSTRACT

Using Rotorcraft Unmanned Aerial Vehicles to deliver supplies to forward ground units in high-threat environments can lead to increases in optempo, enlarge the area of operation, and significantly reduce risk by eliminating pilot safety considerations. The goal of the work presented here was to develop and flight test full flight envelope inner-loop control laws for the autonomous version of the Kaman K-MAX® helicopter. The work included the identification of bare-airframe mathematical models of the aircraft from flight data and combining them with a Simulink® representation of the control laws to develop a detailed analysis model. This analysis model was then validated against closed-loop flight test data and used to generate optimized control system gains for hover and forward flight, at both low and high altitudes. These gains were flight tested through representative mission scenarios and shown to provide improved mission performance.

NOMENCLATURE

BURRO	Broad-area Unmanned Responsive Resupply Operations
GM	Gain margin
H60U	High-altitude 60 kts Unloaded
HHVU	High-altitude Hover Unloaded
L60U	Low-altitude 60 kts Unloaded
LHVU	Low-altitude Hover Unloaded
NLOS	Non-Line of Sight
PM	Phase margin
SCAS	Stability and control augmentation system
UAV	Unmanned Aerial Vehicle
UGV	Unmanned Ground Vehicle
A	Stability derivatives matrix
a_z	Normal acceleration
B	Control derivatives matrix
δ_{col}	Collective control input
δ_{lat}	Lateral control input
δ_{lon}	Longitudinal control input
δ_{ped}	Pedal control input
K_{axis}	Altitude effect on-axis gain
p	Roll rate
q	Pitch rate
r	Yaw rate
u	Control vector
$\dot{v}$	Time derivative of lateral body speed
x	State vector

Presented at the American Helicopter Society 67th Annual Forum, Virginia Beach, VA, May 3-5, 2011.

INTRODUCTION

BURRO (Broad-area Unmanned Responsive Resupply Operations) is an unmanned autonomous external load delivery system based on the K-MAX® helicopter (Figure 1). It is operator-controlled from one or multiple ground control station(s) via RF datalink to the air vehicle. It can be programmed to fly a course of GPS waypoints, including delivering loads at up to four of those points. It has the capability of delivering either single loads, using a single-hook external line, or up to four loads in any combination, using a four-hook carousel, to up to four separate delivery locations in a single sortie. It operates using a fully-redundant flight control system for high reliability and has demonstrated increased endurance using an additional fuel tank in the internal cargo bay, or very long endurance using an external conformal tank.

BURRO development began in 1997 (Figure 2) as a U.S. Marine Corps (USMC) demonstration program to demonstrate unmanned external load stabilization. A ground station was added as part of the system, as well as a rudimentary ability to fly autonomously a course of GPS waypoints, including the ability to autonomously deliver an external load at a specified waypoint. A four-hook carousel was later added, and with it the ability to deliver external loads to up to four independent locations. Finally, autonomous takeoff and landing was added, as well as multiple ground stations. An initial capabilities demonstration was done in January 2001 at Quantico, VA.

Subsequently the Army took over the development efforts and a number of new capabilities were demonstrated: In 2003, BURRO flew the "UAV Corridor" that was being developed from Eglin AFB, FL, to Ft. Rucker, AL. It subsequently demonstrated a NLOS "Netfires Box" placement mission at Ft. Eustis, VA. In 2005, working with the Aviation and Missile Research Development and Engineering Center (AMRDEC) and SAIC, BURRO completed demonstrations of UGV insertion and extraction and multiple load deliveries. In 2006, using an external conformal fuel tank, BURRO demonstrated an unrefueled endurance of 12 hr 17 min. In 2007, development of a dual-redundant flight control system was initiated, and culminated in a fully redundant flight control system being demonstrated in 2009. Development continued through 2010, focusing on high-altitude performance and incorporation of an advanced mission manager and ground station. This system was used for the USMC Immediate Cargo UAS demonstration in early 2011.

This paper presents the latest flight control law improvements undertaken jointly by Kaman and the Aeroflightdynamics Directorate (AFDD) of the U.S. Army AMRDEC in order to optimize the performance of the unmanned K-MAX® for currently planned operations. Previous modeling and control law development efforts were documented in References 1-3. Colbourne, et al (Ref. 1) presented the development of identified state-space models for low-altitude hover, both unloaded and loaded, and described the initial development of unloaded hover control laws. Frost, et al (Ref. 2) continued this work and presented the analyses and optimization of unloaded hover control laws including limited flight testing of the final system. Further details and results of flight testing these control laws were documented by McGonagle (Ref. 3),

Figure 1 – Kaman K-MAX®

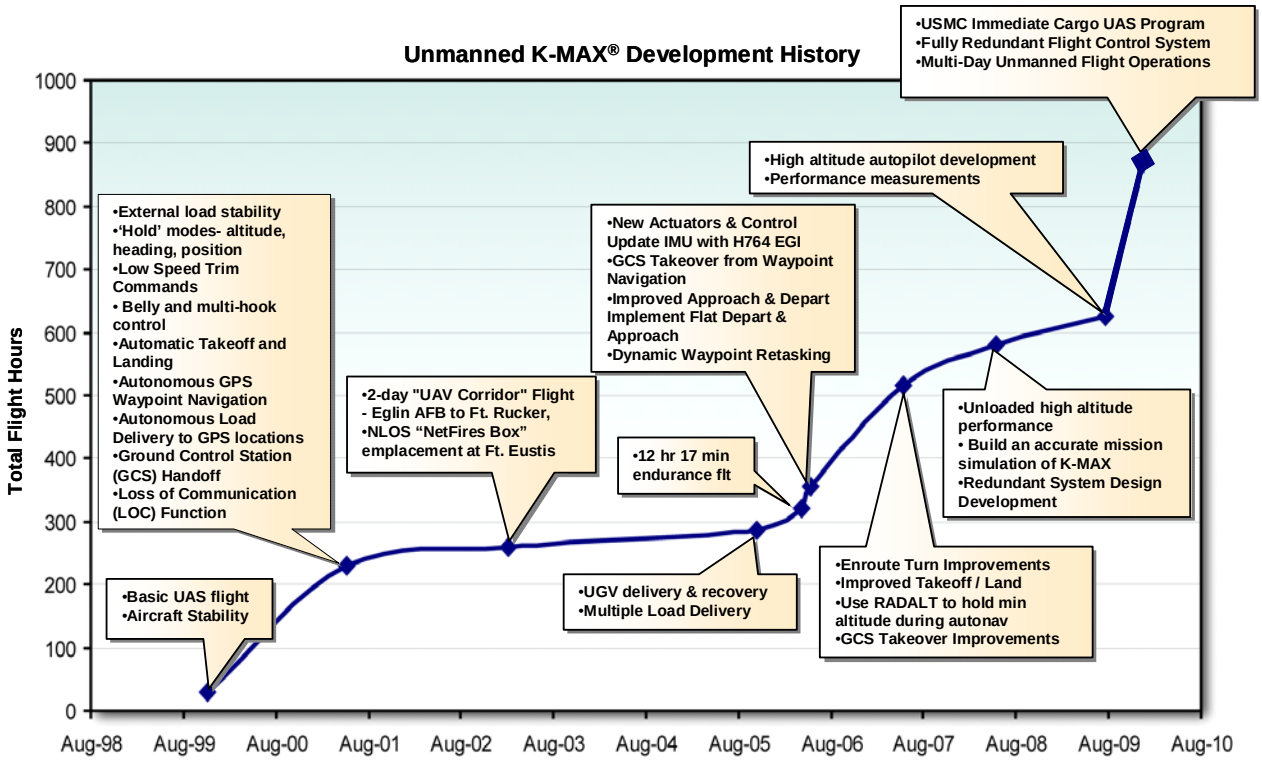

Figure 2 – Unmanned K-MAX® development history

including the incorporation of cable angle feedback to improve stability for external load operations. The current work expanded these previous efforts to cover the entire operational flight envelope of the K-MAX®.

In the current effort, new bare-airframe identified models of the aircraft were developed for hover and forward flight in both low and high altitudes. These were combined with a Simulink® representation of the control laws to create a detailed analysis model for the aircraft. This analysis model was then validated against flight data and optimized to generate control law gains. Only unloaded models and gains were generated. Loaded control law gains were calculated using a priori knowledge of the changes in the flight characteristics of the aircraft while carrying a slung load. Based on the optimized control law gains at each design point, a schedule of gains as a function of airspeed and altitude was developed. This schedule of gains was implemented on the aircraft, flight tested, and shown to result in desired performance and mission capability.

The paper outlines the development of identified state-space models for the K-MAX®, the implementation of the inner-loop control laws in Simulink®, and the combination of these two parts in the Control Designer's Unified Interface (CONDUIT®, Ref. 4-5), along with models of the actuators and sensor filters, to generate a high-fidelity analysis model for the aircraft. The paper then discusses the validation of the analysis model using flight data collected specifically for that purpose. Finally, the optimization of the control laws in CONDUIT® is discussed followed by a brief overview of the results of the mission flight tests.

FLIGHT DATA COLLECTION

A comprehensive flight test program was carried out at the Kaman facility in Bloomfield, CT, during May-August 2010 to gather flight test data specifically for further modeling and flight control improvements. The new flight test program was made necessary because of the expanded flight envelope being considered, and because aircraft hardware changes (e.g. modified torsion stiffness of rotor blades), had made the original flight test data (from 1999) insufficient.

Piloted low- and high-altitude unloaded frequency sweep and doublet tests, as well as automated sweep tests, were carried out in hover and forward flight. Piloted sweep data were collected with the SCAS off for use during frequency-domain bare-airframe model identification. The corresponding SCAS-off doublet data were collected for time-domain validation of the identified models with data not used in the identification process. Finally, the automated sweep data were collected with the SCAS on to allow validation of the control-laws-only implementation, the broken loop responses of the complete analysis model (bare-

airframe, control laws, actuators, and sensors), the associated stability margins, and the closed-loop responses.

Figure 3 depicts an overview of the setup used for collecting automated frequency sweeps in flight. In each axis, the sweep input (r) was added to the output of the control laws upstream of the actuator (f). The sweeps were introduced one axis at a time with the control laws active and the pilot was asked not to add any control inputs unless deemed necessary for safety. Using the resulting data, the control-laws-only (f/y) and broken-loop (f/e) frequency responses were calculated for each axis and used to validate the analysis model, as will be discussed in the "Analysis Model Development and Validation" section later in the paper.

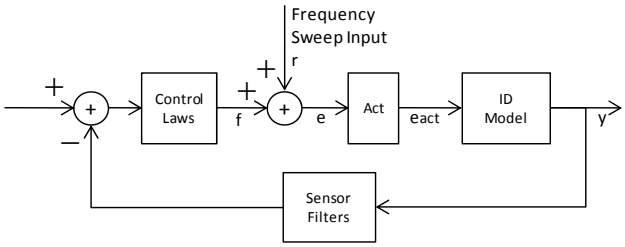

Figure 3 – Relevant parameters for calculating control-laws-only and broken-loop responses

BARE-AIRFRAME MATHEMATICAL MODEL IDENTIFICATION

The first step in developing control laws for any aircraft is the development of accurate bare-airframe mathematical models of that aircraft at all configurations and flight conditions of interest. K-MAX® model identification (using the Comprehensive Identification from FrEquency Responses tool, CIFER®, Ref. 6) was completed for low-altitude hover unloaded (LHVU), high-altitude hover unloaded (HHVU), low-altitude 60 kts unloaded (L60U), and high-altitude 60 kts unloaded (H60U) conditions.

Figure 4 compares the responses of the high-altitude 60 kts unloaded (H60U) model with flight data in the frequency domain. As may be seen the match between the model and flight data is excellent for all primary on-axis responses p/δ_{lat}, q/δ_{lon}, r/δ_{ped}, a_z/δ_{col}. Even the secondary on-axis responses a_z/δ_{lon} and $\dot{v}/\delta_{ped}$ match very well. Figure 5 presents the same comparison in the time domain, using doublet data not used in the identification process. Again, the match can be seen to be excellent. This is also indicated by the excellent overall time-domain cost functions presented in the figure, which are 0.42, 0.38, 0.67, and 0.42 for lateral, longitudinal, directional, and heave respectively (a cost function smaller than one indicates an excellent match, Ref. 6).

The same general level of model identification accuracy was achieved for the other 3 identified models (LHVU, HHVU, L60U). Table 1 summarizes model accuracy results based on frequency domain cost of fit for individual on-axis responses, and for the overall model (average over all responses). Generally, a cost under 100 is considered an acceptable match between model and flight (Ref. 6) and as may be seen from Table 1, all but one of the individual response costs, and all the average costs, are less than 100.

For certain flight segments, for example in climbs and descents, frequency sweep flight data were not collected and rigorous identification was not attempted. However, enough flight data from general mission flights were available to allow simple scale factors to be calculated to modify steady-level models for analysis of climbs and descents. These scale factors were implemented as part of the bare-airframe models that were used in the flight control design process.

ANALYZING THE EFFECT OF ALTITUDE

In all previous work (Ref. 1-3) only flight data at low altitude were available and therefore only models at low altitude were generated. With the complete set of flight data collected for the current development, it was possible to generate models at high altitude as well. However, often it is necessary to use available models to estimate models for conditions for which direct data is not available, for example estimating high-altitude models based on available low-altitude models and intermediate conditions. Having collected a complete data set for this effort it was possible to compare high- and low- altitude data in both hover and forward flight and determine if simple corrections to models at low or high altitude can be used to estimate models for the other flight condition. Figure 6 compares the on-axis roll and pitch responses of the K-MAX® in hover at low altitude with the same responses at high altitude. As may be seen the change in the characteristic of both on-axis responses is confined to a comparable downward shift of the gain curve with no noticeable change in phase. This same general trend was also seen for both the directional and heave axes in hover and for all axes in forward flight (comparing low and high altitudes).

In order to quantify these results, for each axis and flight condition (hover or forward flight) the high-altitude on-axis frequency response was divided by the corresponding low-altitude frequency response and fitted with a gain and a time delay. This was done in CIFER® using the transfer function fitting program NAVFIT. Table 2 summarizes the results including the cost of the fit (fit costs below 50 are considered excellent, Ref. 6). As may be seen from the table, fit costs are generally very low and indicate that on-axis response changes from low to high altitude can be

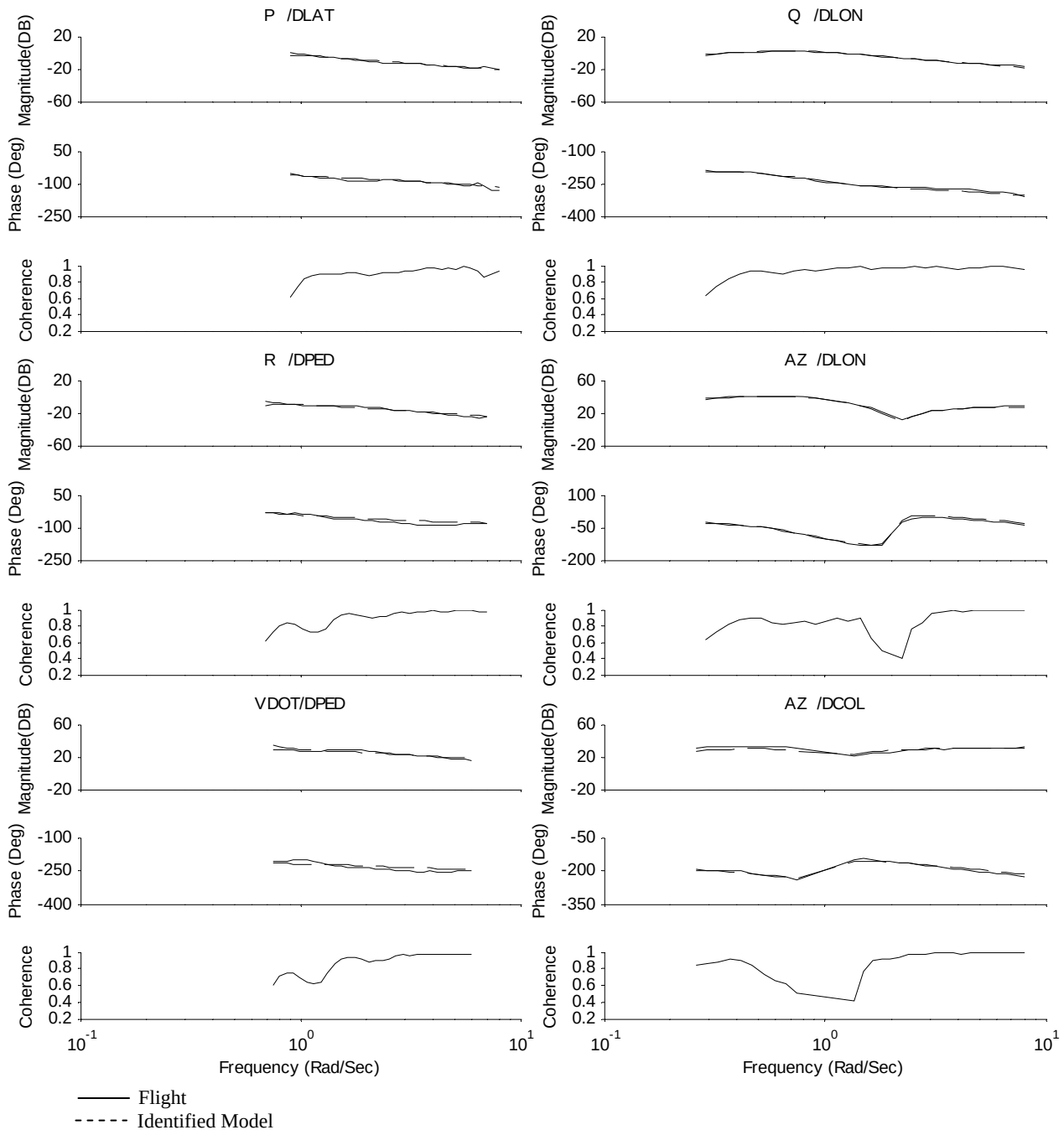

Figure 4 – Frequency-domain validation of the high-altitude 60 kts unloaded bare-airframe ID model

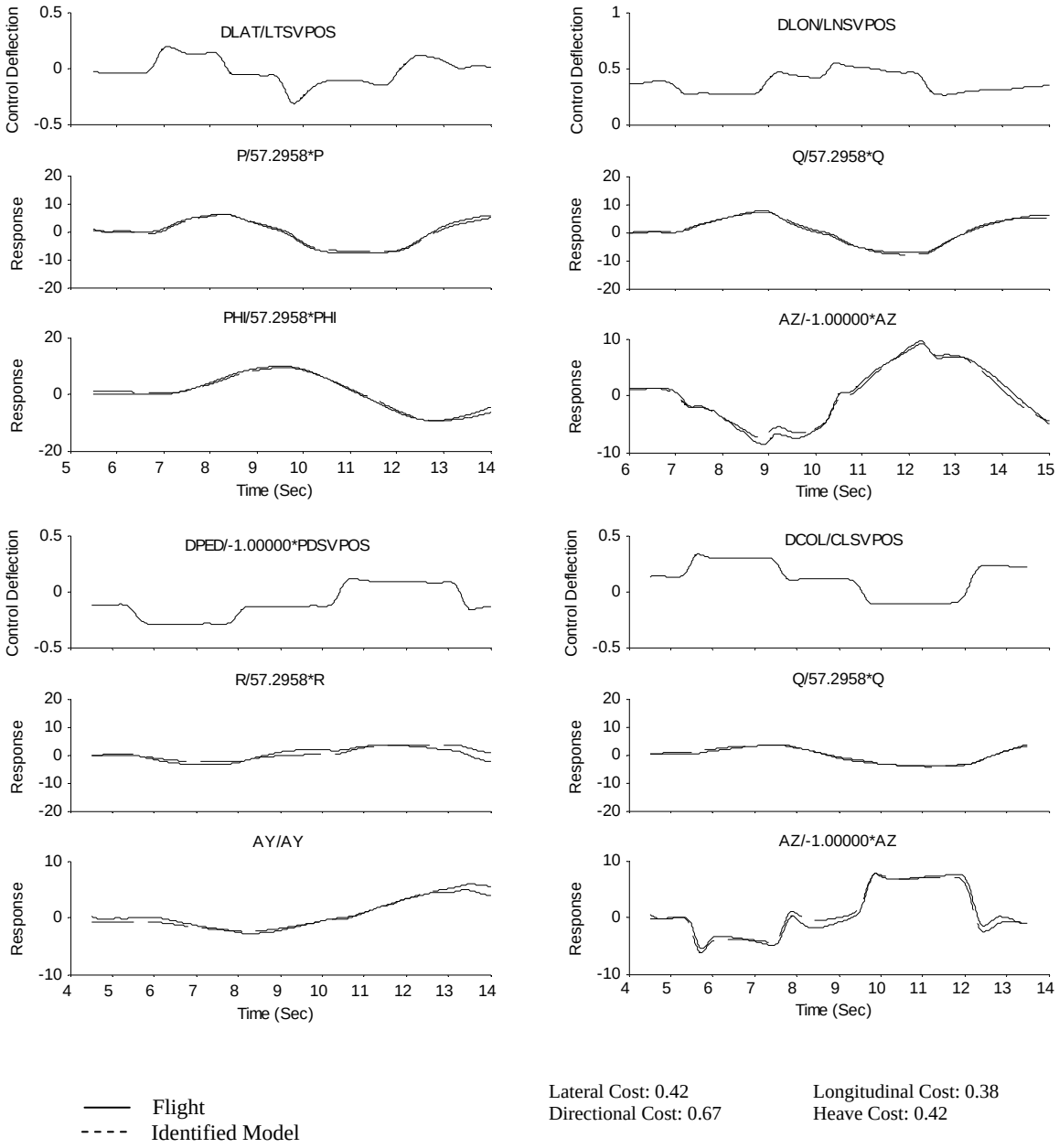

Figure 5 – Time-domain validation of the high-altitude 60 kts unloaded bare-airframe ID model

Table 1 – Primary on-axis and overall average frequency-domain bare-airframe model fit costs

		LHVU	HHVU	L60U	H60U
Individual cost for primary on-axis responses	p/δ_{lat}	74.2	111.4	25.3	66.0
	q/δ_{lon}	79.5	26.7	18.6	17.8
	r/δ_{ped}	65.1	50.4	28.8	32.4
	$\dot{w}/\delta_{col}$	15.2	49.7	23.6	39.4
Average cost for all on- and off-axis responses		56.0	99.4	36.6	46.4

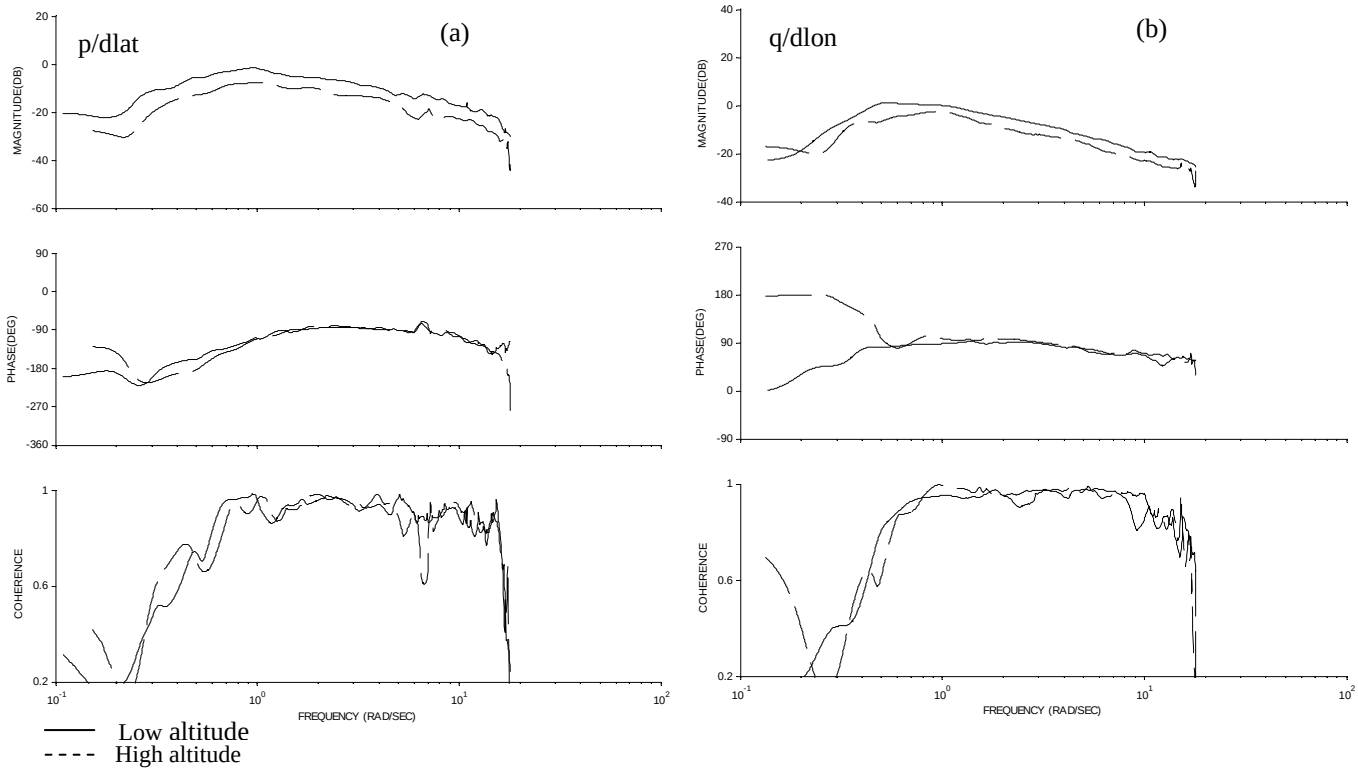

Figure 6 – Effect of altitude at hover, (a) roll rate response to lateral cyclic, (b) pitch rate response to longitudinal cyclic

accurately modeled using a gain and a time delay. Additionally, the table shows that the on-axis response gain change from low to high altitude remains generally the same between hover and forward flight, suggesting that a single altitude correction for each axis can be used for the entire speed envelope, if necessary. Finally, the results show that for most cases the time delay used in the fit is small, as would be expected based on the fact that Figure 6 showed only very small variations in phase. These results suggest that it should be possible to estimate a reasonable high-altitude model using the corresponding low-altitude model in cases where enough high-altitude data is not available for model development. To verify this, scaled high-altitude models were generated using the corresponding low-altitude models by solely using the gains presented in Table 2 as scale factors on the four control inputs. The exact process is outlined in Equations 1-3.

Table 2 – Gain and time delay fit of ratio of high to low altitude on-axis responses

	Fit Range (rps)	Gain HHVU/LHVU	Time Delay LHVU/HHVU	Cost HHVU/LHVU	Gain H60U/L60U	Time Delay H60U/L60U	Cost H60U/L60U
Lateral	1-10	0.532	0.008	33.9	0.656	0.025	34.2
Longitudinal	1-10	0.645	0.002	17.6	0.651	0.002	31.8
Directional	1-8	0.633	0.077	24.1	0.729	0.013	31.1
Heave	2-10	0.481	0.010	16.15	0.460	0.007	34.7

$$\dot{x} = Ax + Bu \tag{1}$$

$$A_{high} = A_{low} \tag{2}$$

$$B_{high} = B_{low} \begin{bmatrix} K_{col} & 0 & 0 & 0 \\ 0 & K_{lon} & 0 & 0 \\ 0 & 0 & K_{lat} & 0 \\ 0 & 0 & 0 & K_{ped} \end{bmatrix} \tag{3}$$

The resulting scaled models for high altitude were then validated against the same high-altitude doublet flight data used for validating the actual identified high-altitude models. The validation results are shown in Table 3 in terms of match cost (J_{RMS}, Ref. 6). Match costs for the actual high-altitude models are also shown for comparison. As expected, the rigorously identified high-altitude models had lower match costs than the scaled models. However, even the scaled models had costs that are considered good (a time-domain cost of 1-2 is considered acceptable), indicating that in the absence of high-altitude data the scaled models could have been a reasonable substitute.

Table 3 – Comparison of match costs for identified and scaled high-altitude models (1-2 considered acceptable)

	High-Altitude Hover Unloaded		High-Altitude 60 kts Unloaded	
	Identified	**Scaled**	**Identified**	**Scaled**
Lateral	0.52	0.91	0.59	1.52
Longitudinal	0.67	0.87	0.54	1.33
Directional	0.31	0.49	0.62	2.52
Heave	0.56	0.86	0.43	0.78

AUTONOMOUS K-MAX® INNER-LOOP CONTROL LAWS

The inner loop control laws for the autonomous K-MAX® perform the automatic stabilization functions and act on commands and moding signals from the outer-loop control laws which perform the autonomous navigation functions (not covered in this paper). Response characteristics are tailored based on mission segment while taking into account loading and altitude considerations. The primary modes in hover are ground speed command for pitch and roll, heading command for yaw, and altitude hold for heave. A position hold capability is implemented in parallel with the ground velocity command loop and both are wrapped around an attitude command core. In forward flight the longitudinal axis retains velocity command functionality while the lateral axis becomes an attitude command system and the directional channel is tuned to maintain coordinated turns. The vertical axis retains altitude command functionality in normal forward flight operations. In addition to these core modes, the control laws implement many special modes designed for specific segments of flight, including automatic take-off and landing and rapid climbs and descents, to name a few. These will not be directly addressed in this paper. Figure 7 provides a top level overview of the inner-loop control laws for the unmanned K-MAX® (highly simplified longitudinal hover unloaded portion shown).

ANALYSIS-MODEL DEVELOPMENT AND VALIDATION

The analysis model combines the bare airframe identified models and a detailed Simulink® representation of the control laws, and is implemented using CONDUIT®. The control laws, as implemented in the CONDUIT® case, account for all modes of operation from hover to forward flight. The "Bare Airframe ID Model" block shown in Figure 7 was implemented such that all four identified models were included and the appropriate one could be selected based on regime of flight being analyzed. In conjunction, appropriate switchologies were included to allow proper modes and control law paths to be selected, again based on regime of flight.

Prior to conducting any analysis and optimization, it is important to ensure that the analysis model is an accurate

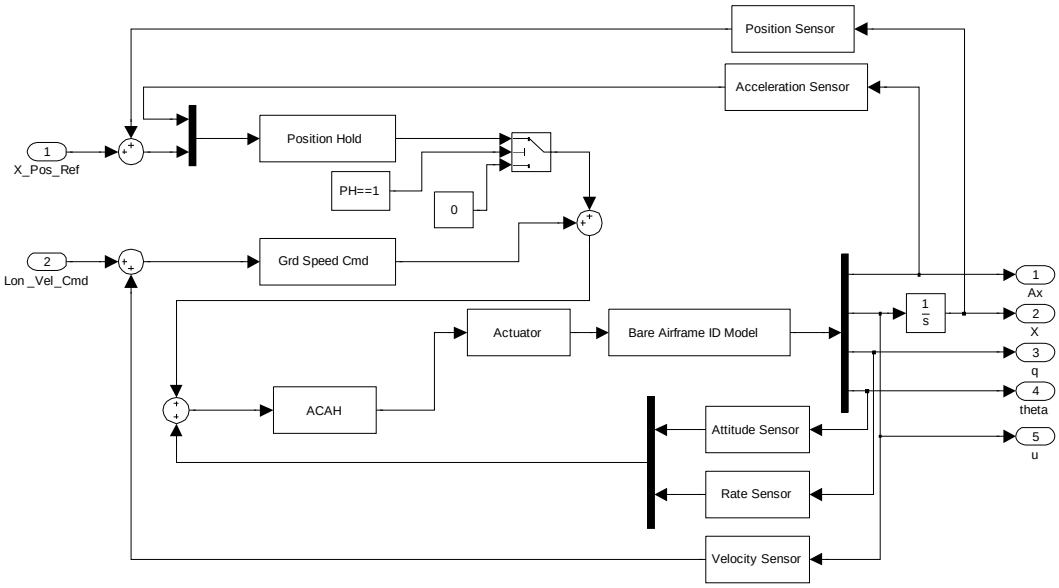

Figure 7 – Overview of the inner-loop control laws (simplified longitudinal hover unloaded shown)

representation of the actual flying vehicle. Both time- and frequency-domain validations were performed, using mission and automated sweep flight data, to confirm the accuracy of the analysis model.

Since many of the internal control law parameters, in addition to the aircraft-state feedback parameters, were recorded and made available in the collected flight data, a very detailed validation of the control laws portion of the analysis model, including the sensor filters, could be carried out. The Simulink® block diagram was set up so that for each control law signal for which flight data was available, an input port was added to allow flight data for that signal to be fed in. An output port was also added for the same signal so that the simulated signals could be recorded. Additionally, ports were added to certain integrator blocks to allow proper alignment of integrator initial conditions for validation purpose. Finally, proper logic gates were implemented to account for correct mode switching when playing back the flight data through the control system. This set up provided an organized and effective mechanism for validating every key signal path of the control laws. For each axis, starting from the beginning of the feedback path of the control laws, flight data was systematically fed into a current signal port, and the simulated output signal of the port immediately downstream was recorded and compared against the flight data. Ultimately, only the aircraft-state feedback parameters were fed into the control laws, and the signals at the actuator inputs were compared against flight data to ensure that the end-to-end responses of the control system matched the flight data accurately.

To facilitate this comprehensive validation of the control laws, the Analysis Tools in CONDUIT® was employed. The Analysis Tools (Ref. 5) provides a graphical user interface which automatically scans and compiles a list of all the signal paths in the block diagram, and presents the list as a drop-down menu for easy selection of the signal path to be examined. The tool also provides a comprehensive plotting environment to allow overlaying of simulated signals against flight data. Using Analysis Tools, the process of conducting time-domain validation of the control laws was greatly simplified and streamlined, and the end-to-end validation was performed much more rapidly than would have been possible otherwise.

Figure 8 compares the end-to-end control-laws-only outputs of the CONDUIT® analysis model with flight data for the low-altitude hover unloaded case. Here, the aircraft state measurements (e.g., $p, q, r, \phi, \theta, a_{y,}$ etc) were fed into the control laws and the resulting actuator command for each axis compared to flight test data. For the longitudinal and lateral axes, the control laws were in position hold mode, whereas for the directional and heave axes the control laws were in heading hold and altitude hold mode, respectively. The figure shows that the CONDUIT® implementation is a very close representation of the control laws as implemented on the aircraft and can be relied upon for analyses and optimization.

With the control-laws-only portion of the analysis model successfully validated in the time domain, the same automated sweep data were used for the validation effort in

the frequency domain. The data were processed through CIFER® to generate frequency responses for the control laws and these were compared with the responses of the analysis model. Similar to the time domain validation effort, the comparisons were carried out using the Analysis Tool and the results showed very good matches between analysis and flight. Frequency responses were also generated to validate the actuator representations, which were modeled as second order systems with rate and position saturation limits to capture the proper non-linear dynamics, and results indicated the actuator models to be very accurate.

Once the control laws and the actuator models were successfully validated, the final step was to validate the entire analysis model, which included the identified bare airframe models, the actuator models, the control laws, and the sensor filters. Broken-loop validations, which provide the most complete look at the accuracy of the analysis model, were performed. Figure 9 depicts an example of such a comparison for the low-altitude hover unloaded case.

Figures 9a and 9b show the comparison of the analysis model with the flight data for the lateral and longitudinal axes, respectively, in velocity command mode. It can be seen that in both cases the broken-loop responses match very well in the frequency range of 1 to 10 rad/sec, which is the frequency range of primary concern for flight control analysis and for which good coherence was achieved. With such good agreements, accurate crossover frequencies and stability margins can be determined from the analysis model. Similarly, Figure 9c compares the directional broken-loop responses in heading hold mode. Again, both the magnitude and phase appear to be quite accurate for the frequency range of interest, though there seems to be a slight under prediction of the effective time delay by the analysis model.

Finally, Figure 9d compares the broken-loop responses for the heave axis in altitude hold mode. The match between the analysis and flight is quite good below 2 rad/sec. It was determined that the mismatch beyond 2 rad/sec was primarily due a software rate limit in the collective feedback path which was reached during the frequency sweep flight tests. Software nonlinearities in general were not accounted for in the linear analysis, resulting in the discrepancy observed. Note, however, that certain critical nonlinearities, such as actuator rate limits, were accounted for in the linear analysis through specialized specifications such as the Open-Loop Onset Point (OLOP) specification (Ref. 7).

To confirm that software rate limiting was indeed the primary source of the discrepancy observed in the heave axis broken-loop comparison, frequency sweeps were injected into the analysis similar to the way it was done for the automatic sweep flight tests (Figure 3). Time histories of the control law servo command and the actuator input (signals f and e in Figure 3, respectively) were recorded in Analysis Tools, and the broken-loop response was generated using CIFER®. The response was overlaid in Figure 9d to compare against the broken-loop responses from both CONDUIT® (linear analysis) and flight data. It can be seen from the magnitude plot that the frequency response based on the sweep input has correctly captured the dynamics of the software rate limiting effect, thus confirming the source of the observed discrepancy. It can also be seen from the phase plot that the sweep-input-based broken-loop response contains approximately an additional 40 msec of time delay at high frequencies. Despite the observed discrepancies, all three heave broken-loop frequency responses match quite well in the region of crossover, and therefore the phase margin calculation should be quite accurate.

In summary, the results of both time- and frequency-domain validations indicated that the analysis model was an accurate representation of the actual aircraft and could be reliably used for analysis and optimization.

CONTROL LAWS OPTIMIZATION

The control laws were optimized in CONDUIT® against a set of stability and performance specifications designed to ensure adequate margins while providing best possible performance within the maneuvering capabilities of the aircraft (Ref. 8). Non-linearities, such as actuator rate limits, were included so that the resulting gains would provide the expected performance for the actual system. All control laws paths were independently and collectively analyzed in various modes of flight. For example, even though the aircraft is never flown directly in longitudinal attitude command mode, specifications, including the longitudinal attitude bandwidth specification from ADS-33 (Ref. 9), were included in the analyses and optimization. Since the inner attitude command loop acts as an actuator for the outer velocity and position loops, adequate margins and good performance of the attitude path is necessary for achieving the desired stability and performance goals in velocity command and position hold.

Overall stability was ensured by using eigen-location specifications which force all closed-loop system poles to be at least neutrally stable. In conjunction, eigen-damping specifications were used to ensure that all closed-loop short term response poles had a damping ratio of at least 0.35. Additionally, satisfactory margins were guaranteed in all axes by using stability margin specifications which look at the broken-loop responses of the system. These were implemented both at the actuators and at outer summing points of the loop being considered, since margins at these two points can be different.

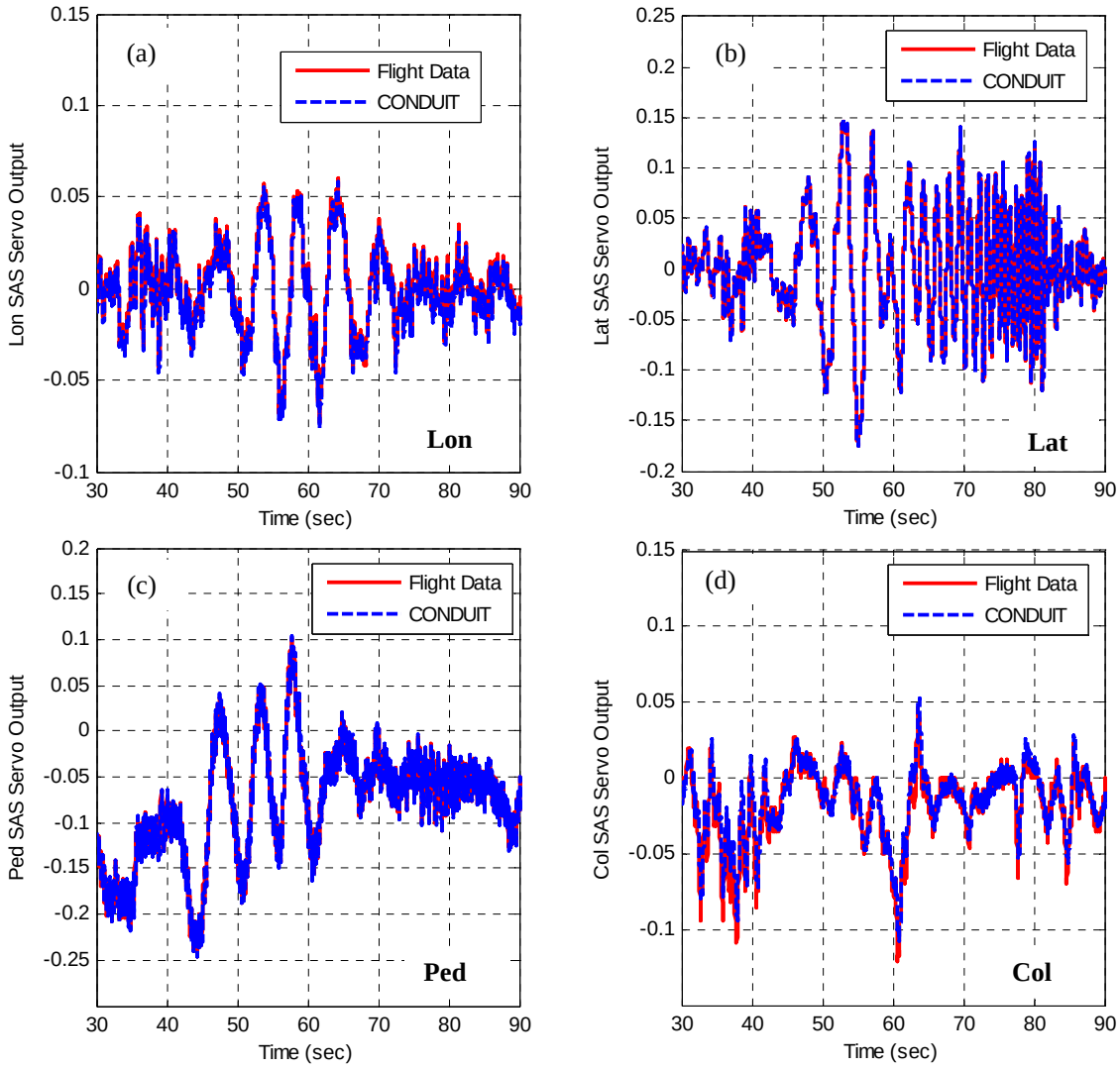

Figure 8 – Time-domain comparison of control-laws-only portion of the analysis model for low-altitude hover unloaded

The key measure of performance included in the analyses and optimization was the disturbance rejection bandwidth (DRB) specification (Ref. 10) which was included for attitude, velocity, and position in pitch and roll, and for heading and altitude in yaw and heave respectively. In every case the DRB specification was accompanied by a corresponding disturbance rejection peak (DRP) specification which controlled response overshoot and oscillatory behavior (Ref. 8). Note that since the primary mission of the autonomous K-MAX® is to carry an externally slung load, the desire for high DRB had to be tempered to ensure that the resulting motions of the aircraft would not be too abrupt and cause undesirable swinging of the load. This was accomplished by using more conservative boundaries on the DRB specifications. To prevent these lower allowable DRB boundaries from lowering the crossover frequencies and negatively affecting robustness, minimum crossover frequency specifications were used in all loops.

As mentioned previously, closed-loop automated frequency sweep flight data were used to generate accurate models of all four actuators. These models, coupled with the Open Loop Onset Point (OLOP) specifications (Ref. 7), were used in all axes so that the optimized gains would not result in excessive actuator rate saturation and limit cycle behavior.

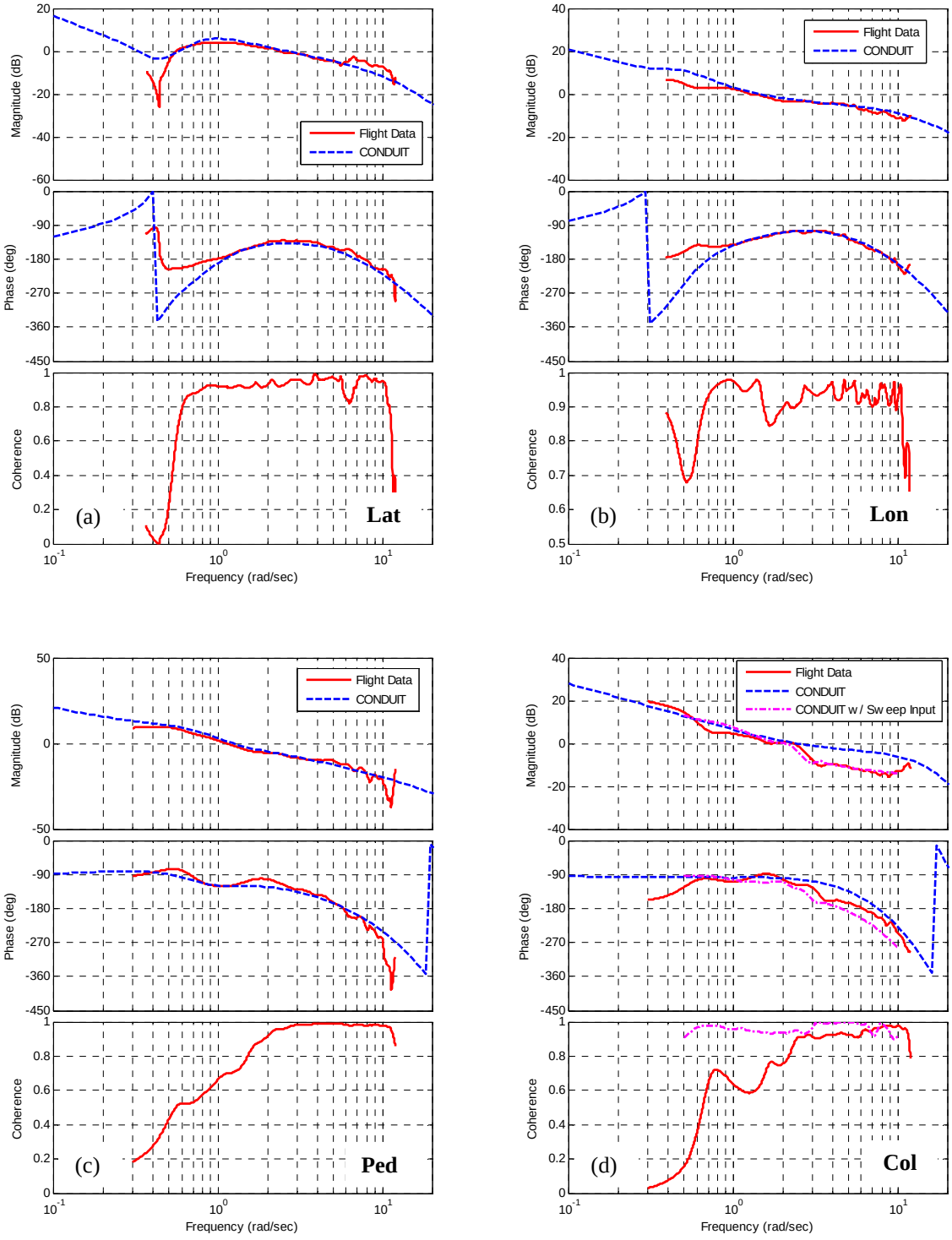

Figure 9 – Broken-loop frequency response comparisons for lateral (velocity command), longitudinal (velocity command), directional (heading hold), and heave (altitude hold) in low-altitude hover unloaded

Optimizations were carried out for the four flight conditions mentioned earlier and the resulting control system gains were incorporated in a bi-variate table of gains, as a function of airspeed and altitude, and used during evaluation flight tests. Gain variations as a function of load were implemented as adjustments applied to gains calculated from this bi-variate table. Figure 10 presents an example optimization result for the high-altitude 60 kts unloaded case, depicted on the CONDUIT® HQ window. Note that many more specifications were used in the actual optimizations and only an abbreviated version of the HQ window is shown here for illustration purposes. As may be seen from Figure 10, all specifications are satisfied to Level 1 (blue region, satisfactory without improvement). More explanation of the CONDUIT® specifications and HQ window are given in Ref. 4 and Ref. 8. A few key results can be noted as follow, with the relevant specification marked with a number corresponding to items in the list below:

1. Stability and adequate damping were achieved, as indicated by the location (EigLcG1 spec) and the minimum damping (EigDpG1 spec) of all closed-loop system poles. Additionally, stability margin (StbMgG1) and Nichols margin (NicMgK1) specifications showed that the system possessed desirable and robust stability margins.

2. Adequate stability margins were achieved even in the presence of modes that may not have been accurately captured by the ID models. This was accomplished by using, in addition to the standard stability margin specifications, specialized stability margin specifications (StbDaG1) which use frequency responses from actual flight data for the bare-airframe (Ref. 11, 12).

3. There is only a very low probability of encountering actuator rate saturation, as seen from the Open Loop Onset Point specifications (OlpOpG1) being deep in Level 1.

4. The aircraft response to a velocity command is reasonably fast, as shown by the rise time specification (RisTmG1), without being overly aggressive or causing actuator rate saturation. As mentioned before, the desire for high performance had to be tempered by a need to prevent abrupt responses which could result in undesirable load motion.

A look at the variation of the optimized control law gains across altitude would be informative in light of the previously presented effects of altitude on bare-airframe dynamics. The overall effect of the variation of all the free gains and lead-lag compensators on the response across altitude can be examined by comparing the broken-loop responses. Figure 11a shows the lateral broken-loop response of the system in hover under velocity command. As may be seen, the optimized gains for low altitude work well in low altitude and provide a crossover around 2.3 rad/sec with adequate margins (GM = 5.2 dB, PM = 40.7 deg). Taking the same gains to high altitude clearly would result in unacceptable margins, as may be seen from the figure (GM = 0.5 dB, PM = 7.7 deg). The optimized high-altitude gains, however, adjust for the variations in aircraft characteristics and have recovered approximately the same crossover frequency and margins (GM = 6.0 dB, PM = 45.0 deg). As Figure 11b shows, the same is true in forward flight, though the achievable margins at low-altitude are more limited. Finally, the same results are confirmed for the disturbance responses in Figure 12, which show that using the low-altitude gains at high altitude would result in unacceptable peaking of the disturbance response while the optimized high-altitude gains capture nearly the same DRB as in low altitude without excessive peaking. Therefore, it is clear that scheduling with altitude is necessary.

DEVELOPMENT OF FULL-FLIGHT-ENVELOPE STITCHED MODEL

Using the linear bare-airframe models discussed above, and the implementation of the inner-loop control laws in Simulink®, a full-flight-envelope simulation model of the unmanned K-MAX® was developed for desktop flight simulation, full-flight-envelope control system evaluations, and operator training. This full-flight-envelope tool is the most effective means of dynamically evaluating gain schedules and control system mode-transitions as they would happen in flight.

The model stitching technique developed by Zivan and Tischler (Ref. 13) was used for the bare-airframe portion, which necessitated the collection of additional trim flight-test data specifically for this process. To highlight the fidelity of the stitched model, Figure 13 compares the lateral broken-loop response of the stitched model with a constituent linear point model. The figure shows that while the stitched model provides a smooth variation in the aircraft response from hover to high forward speed, it remains nearly as accurate as the linear point models it was derived from at their corresponding identification points.

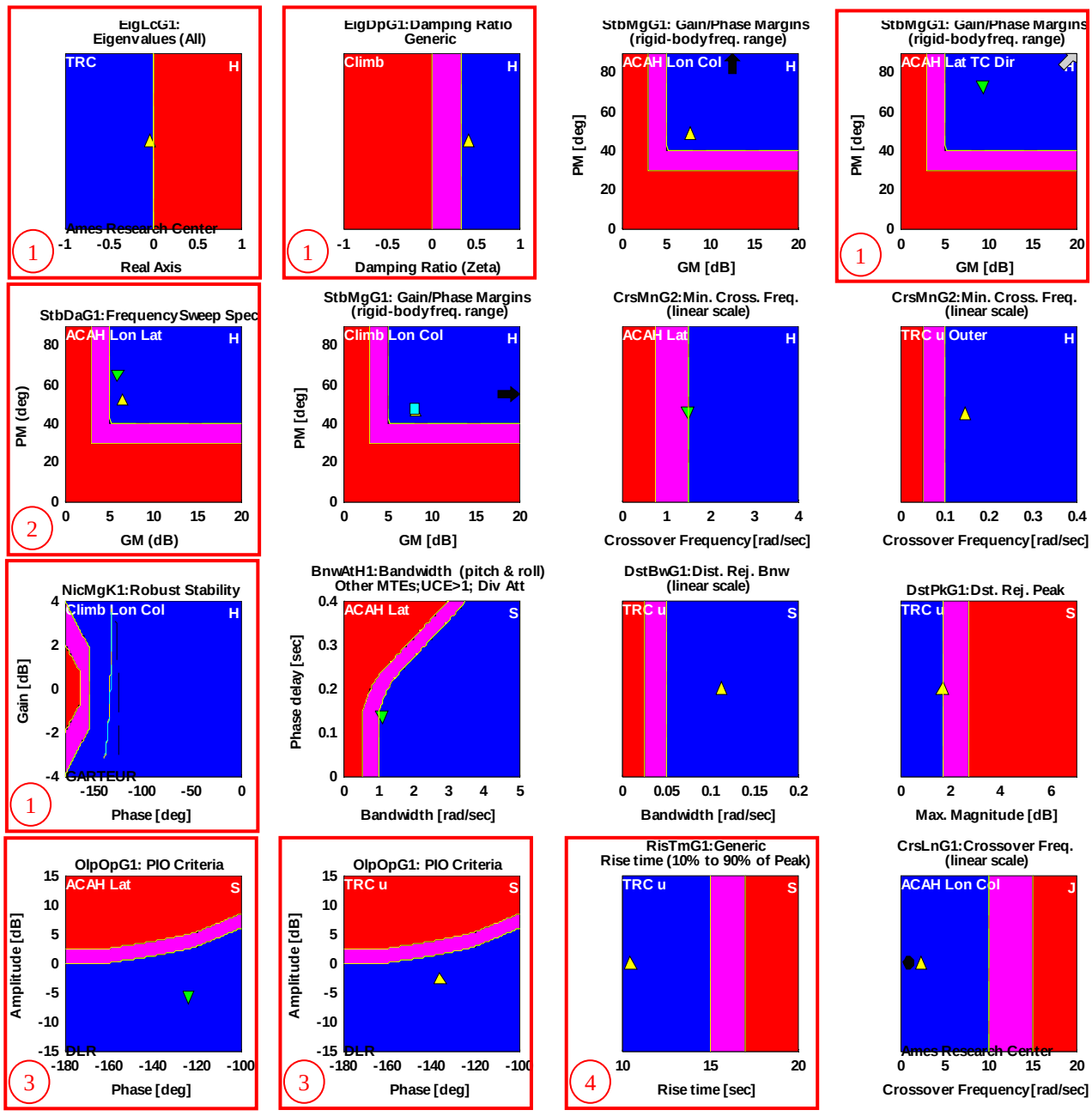

Figure 10 – CONDUIT® HQ window showing high-altitude 60 kts unloaded optimization results

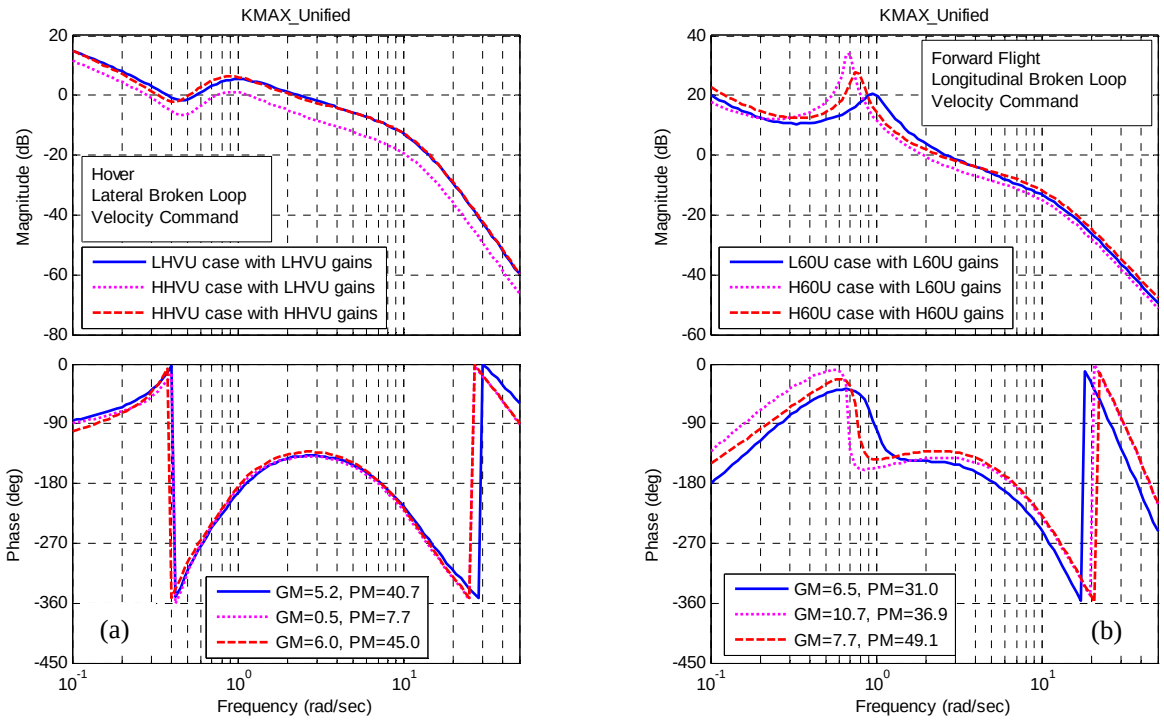

Figure 11 – Broken-loop frequency responses highlighting effect of altitude and need for gain scheduling: a) lateral hover, b) longitudinal forward flight

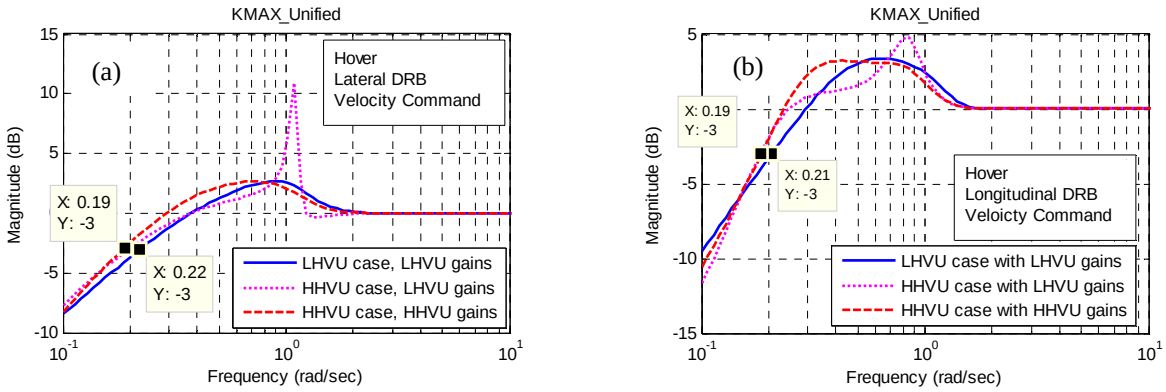

Figure 12 – Disturbance responses highlighting effect of altitude and need for gain scheduling: a) lateral hover, b) longitudinal hover

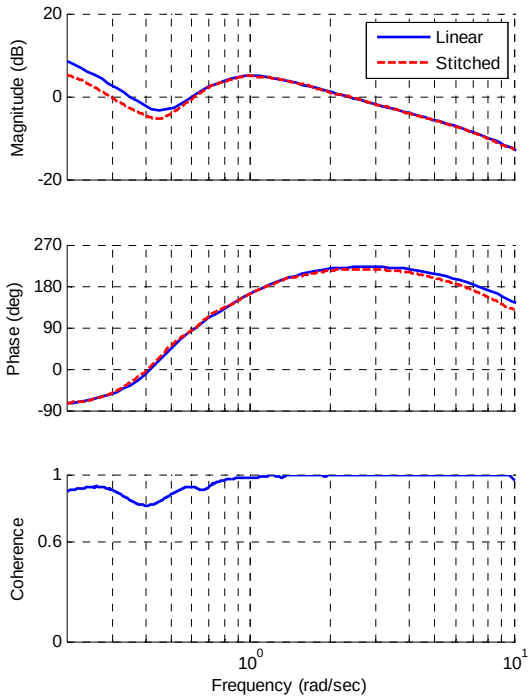

Figure 13 – Stitched model lateral broken-loop response compared to response of constituent point model

FLIGHT TEST EVALUATIONS

As mentioned previously, the control system gains developed for low- and high-altitude hover and low- and high-altitude forward flight were implemented in a bi-variate lookup table, as a function of airspeed and altitude, and implemented on the aircraft. The gain values were clamped to their maximum airspeed and maximum altitude values to prevent undesirable values due to extrapolation. The aircraft was then flight tested across its mission envelope using these gains and shown to perform very well.

The new gains were shown to result in better damping in forward flight, including climbs and descents to and from high altitudes. The safety pilot commented that the system now "actually flies like I would", not chasing airspeed but instead maintaining a stable attitude with small variations in airspeed. Hover stability was shown to have improved, especially in off-nominal conditions such as tail winds. The safety pilot also commented that in higher wind and turbulence conditions the aircraft “rides the bumps” instead of trying to fight them and possibly resulting in undesirable load motion. Generally, the new gains were described as being the most stable to date in high winds and moderate turbulence.

CONCLUSIONS

Optimized control system gains for the unmanned K-MAX® were developed at various flight conditions. The process included collecting flight data for model development and validation, development of bare-airframe identified models, implementation of the control laws in Simulink®, development and validation of a complete analysis model, and optimization of control law gains using CONDUIT®. The resulting gains were successfully flight tested while performing various mission elements. Safety pilot comments and collected data indicated noticeable improvements in mission performance.

REFERENCES

1. Colbourne, J., Cicolani, L., Tischler, M., Frost, C., Tomashofski, C., & LaMontagne, T., "System Identification and Control System Design for the BURRO Autonomous UAV," Proceedings of the American Helicopter Society 56th Annual Forum, Virginia Beach, Virginia, May 2000.
2. Frost, C., Tischler, M., Bielefield, M., & LaMontagne, T., "Design and Test of Flight Control Laws for the Kaman BURRO Unmanned Aerial Vehicle," Proceedings of the American Institute of Aeronautics and Astronautics Atmospheric Flight Mechanics Conference, Denver, CO, August 2000.
3. McGonagle, J., "The Design, Test, and Development Challenges of Converting the K-MAX® Helicopter to a Heavy Lift Rotary Wing UAV," Proceedings of the American Helicopter Society 57th Annual Forum, Washington, D.C., May 9-11, 2001.
4. Tischler, M. B., et al, "A Multidisciplinary Flight Control Development Environment and Its Application to a Helicopter," IEEE Control Systems Magazine, Vol. 19, No. 4, pg. 22-23, August 1999.
5. Anon, "CONDUIT® User’s Guide, Version 5.2," University Affiliated Research Center, Moffett Field, California, October 2010.
6. Tischler, M. B. and Remple, R. K., "Aircraft and Rotorcraft System Identification: Engineering Methods with Flight Test Examples," AIAA, August 2006.
7. Duda, H., "Prediction of Pilot-in-the-Loop Oscillations due to Rate Saturation," AIAA Journal

of Guidance, Navigation, and Control, Vol. 20, No. 3, May-June 1997.

8. Tischler, M. B., Ivler, C. M., Mansur, M. H., Cheung, K. K., Berger, T., Berrios, M., "Handling Qualities Optimization and Trade-offs in Rotorcraft Flight Control Design," presented at AHS Specialists Meeting on Rotorcraft Handling-Qualities, Liverpool, U.K., November 4-6, 2008.
9. Anon., "Handling Qualities Requirements for Military Rotorcraft," Aeronautical Design Standard-33 (ADS-33E-PRF), U.S. Army Aviation and Missile Command, March 21, 2000.
10. Blanken, C. L., Hoh, R. H., Mitchell, D. G., Key, D. L., "Test Guide for ADS-33E-PRF," U.S. Army RDECOM Special Report AMR-AF-08-07, July 2008.
11. Fletcher, J. W., et al, "UH-60M Upgrade Fly-By-Wire Flight Control Risk Reduction using the RASCAL JUH-60A In-Flight Simulator," Proceedings of the American Helicopter Society 64th Annual Forum, Montréal, Canada, April 29 - May 1, 2008.
12. Ivler, C., Tischler, M. B., "System Identification Modeling for Flight Control Design," presented at AHS Specialists Meeting on Rotorcraft Handling-Qualities, Liverpool, U.K., November 4-6, 2008.
13. Zivan, L., Tischler, M. B., "Development of a Full Flight Envelope Helicopter Simulation Using System Identification," Journal of the American Helicopter Society, Vol. 55, No. 2, April 2010.